Konrad-Zuse-Zentrum
für Informationstechnik Berlin

Takustraße 7
D-14195 Berlin-Dahlem
Germany

FRANK SCHMIDT

Computation of Discrete Transparent Boundary Conditions for the 2D Helmholtz Equation

Preprint SC 97-64 (December 1997)

Computation of Discrete Transparent Boundary Conditions for the 2D Helmholtz Equation

Frank Schmidt

Abstract

We present a family of nonlocal transparent boundary conditions for the 2D Helmholtz equation. The whole domain, on which the Helmholtz equation is defined, is decomposed into an interior and an exterior domain. The corresponding interior Helmholtz problem is formulated as a variational problem in standard manner, representing a boundary value problem, whereas the exterior problem is posed as an initial value problem in the radial variable. This problem is then solved approximately by means of the Laplace transformation. The derived boundary conditions are asymptotically correct, model inhomogeneous exterior domains and are simple to implement.

AMS Subject Classification: 65N38, 65N30, 78A45

Keywords: Helmholtz equation, non-reflecting boundary condition, finite element method, Sommerfeld's radiation condition, optical waveguides

1 Introduction

The numerical simulation of wave propagation in integrated optics or fiber optics devices is one of the central tasks in the design and optimization of effective components. Fortunately, many structures like waveguides or tapers can be modeled based on a uni- or bidirectional wave propagation. Simulation tasks of this kind can be solved by a number of different methods, most prominent here are the various types of Beam Propagation Methods (BPM). The central idea of BPM's, from its origin, has been to solve the scalar Helmholtz equation approximately by a reformulation of the boundary value problem as an initial value problem. This concept is close to the working principle of those optics components, which are characterized by a well defined direction of propagation. Some problems, however, require simulation tools which are able to take into account arbitrary directions of wave propagations. For such type of problems it is natural to go back to the scalar Helmholtz equation

$$\Delta u(x,y) + n^2(x,y)k_0^2 u(x,y) = 0, \quad u \in H^1(\Omega), \tag{1}$$

defined on some bounded domain Ω. Here $n(x,y)$ denotes the refractive index geometry of a given structure, k_0 is the wavenumber defined by $k_0 = 2\pi/\lambda$, and λ is the wavelength in vacuum. Equation (1) poses an elliptic boundary value problem. In order to solve it, one needs the incident field along the *whole* boundary together with suitable boundary conditions. Ideally, these boundary conditions should lead to the same solution $u(x,y)$ on Ω, as the one obtained by solving the Helmholtz equation on the whole, infinite domain. Exactly this idea has been proved to be of great practical relevance in simulation of grating structures [1]. As another example consider the configuration given in Fig. 1. The incident light, guided by a waveguide, is reflected by a small dielectric mirror. The dimensions of the mirror are such that besides the reflection refraction and diffraction occurs, too. This example will serve throughout the paper as model problem.

An alternative choice is to solve the corresponding time-dependent wave equation by means of a finite-difference-time-domain (FDTD) method. This approach has been shown to be successful for a general class of structures [2]. It is advantageously, if the response with respect to an arbitrary time-dependent input is analyzed. In the problem class under consideration, however, where a time-harmonic incident wave is given, it is more efficient to solve the problem directly in its time-harmonic form. The central problem arising here is to construct transparent boundary conditions for general smooth boundaries and to find a suitable formulation of the interior problem, which

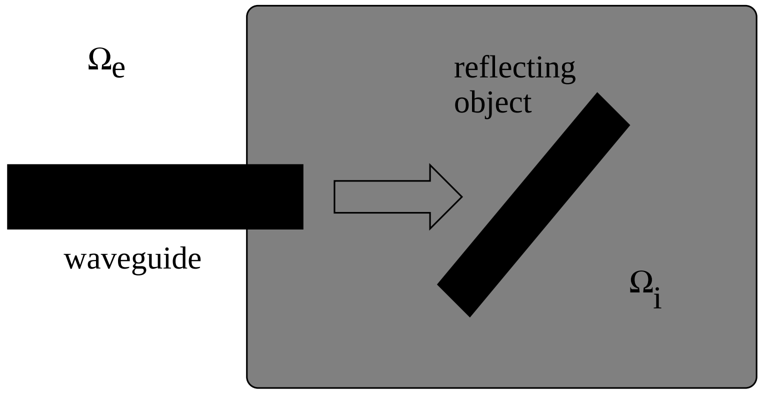

Figure 1: Typical configuration of a reflection problem

allows for a direct implementation of these boundary conditions. Concerning the Helmholtz equation with homogeneous exterior domains, there are a large number of proposals to derive suitable boundary conditions. First, and most important, are the Sommerfeld-like boundary conditions based on Sommerfeld's famous asymptotic boundary condition, [3], $\partial_r u - in_0 k_0 u = o(r^{1/2})$. Then there are the nonlocal Dirichlet-to-Neumann boundary conditions for separable coordinate systems [4] and [5], the family of corresponding local and asymptotic approximations [6], infinite element methods [7] and the various kinds of boundary element methods [8]. However, if the exterior domain becomes inhomogeneous, e. g. by an embedded waveguide (Fig. 1), these methods do not longer work. For such cases GOLDSTEIN [9] offers a solution by constructing transparent boundary conditions valid on a part of the whole boundary. This part of the boundary contains the position where the waveguide hits the boundary and the area surrounding the waveguide. In Fig. 1 this would be the left, vertical part of the boundary. The corresponding boundary conditions are obtained by an eigenmode decomposition of the waveguide assuming Dirichlet boundary condition at the ends of the cut interval.

Our approach is different from these methods. It is based on the numerical methods developed for the time-dependent Schrödinger equation [10, 11]. It supplies a family of asymptotic correct boundary conditions for a large class of interior domains with smooth boundaries and possibly inhomogeneous exterior domains. The main idea is to write the interior problem as a variational problem in standard manner, representing a boundary value problem, whereas the exterior problem is posed as an initial value problem in the radial variable. This exterior problem is similar to the exterior problems discussed in conjunction with the Schrödinger equation in [10, 11]. Therefore we can apply the techniques derived there to construct the transparent boundary conditions by means of the Laplace transformation.

2 Variational Formulation

In standard fashion, we obtain the variational form of (1) by multiplication with a test function $v \in H^1(\Omega)$ and integration by parts

$$-(\nabla v, \nabla u) + (v, n^2 k_0^2 u) = -\int_\Gamma \mathbf{n} v \nabla u \, ds \quad u, v \in H^1(\Omega), s \in \Gamma \quad .$$

Here Γ denotes the boundary and $(v,u) = \int_\Omega \bar{v} u \, dxdy$. The function $u(s), s \in \Gamma$, may be considered as a superposition of incoming and outgoing waves, $u(s) = u_{in}(s) + u_{out}(s)$. Suppose a boundary operator $\tilde{b}(s)$ is given, which relates the normal derivative to the boundary values as

$$\mathbf{n}(s) \nabla u_{out} = \tilde{b}(s) u_{out},$$

with $\mathbf{n}(s)$ the outward normal vector. Then it follows

$$\mathbf{n} \nabla (u_{\text{in}}(s) + u_{\text{out}}(s)) = \mathbf{n} \nabla u_{\text{in}}(s) - \tilde{b} u_{\text{in}}(s) + \tilde{b} u(s) \, .$$

With the reformulation of the boundary operator $\tilde{b}(s)$ in its variational form,

$$b(v,u) = \int_\Gamma \bar{v}(s) \tilde{b}(s) u(s) \, ds \quad v \in \gamma \left(H^1(\Omega) \right) \, ,$$

γ the trace operator $\gamma : H^1(\Omega) \rightarrow L_2(\Gamma)$, we end up with the following variational problem: find $u \in H^1(\Omega)$, such that

$$a(v,u) + b(v,u) = -\int_\Gamma \bar{v} \mathbf{n} \nabla u_{\text{in}} \, ds + b(v, u_{\text{in}})$$

for all $v \in H^1(\Omega)$. Once the continuous variational formulation is obtained, the restriction to the finite dimensional finite element space $V_h \subset H^1(\Omega)$ yields, in the standard way, the corresponding discrete problem

$$(\mathbf{A} + \mathbf{B}) \mathbf{u} = \mathbf{r} \, .$$

The matrix $\mathbf{A}$ is the conventional finite element system matrix of the Helmholtz equation, the matrix $\mathbf{B}$ is the discrete version of the boundary operator and realizes the transparency of the boundary. $\mathbf{B}$ acts only on the boundary nodes. The right hand side vector $\mathbf{r}$ contains the information about the incident wave.

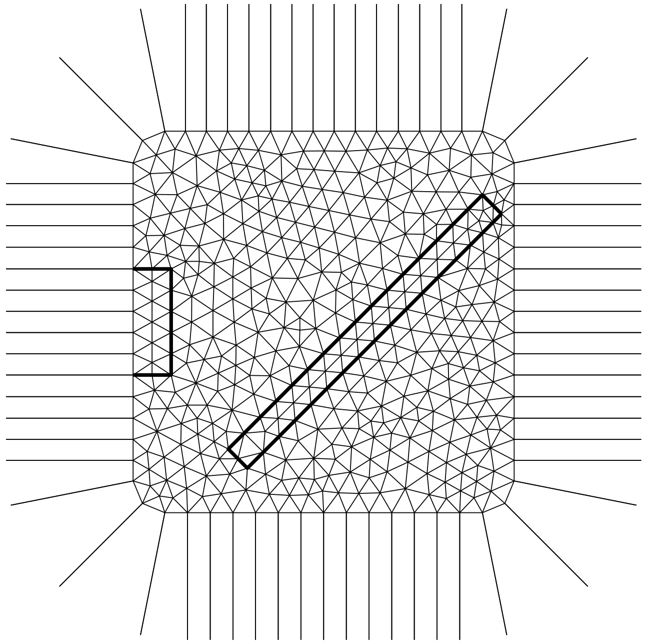

Figure 2: Discretization of the problem. The interior domain is discretized using triangles. The exterior domain is discretized only in the tangential coordinate. Along the rays the solution is approximated semi-analytically.

3 Semi-discretization of the exterior domain

The central question is, how to derive the discrete boundary operator $\mathbf{B}$. To this end, we discretize the whole problem as it is shown in Fig. 2. The triangulation of the interior domain domain supplies a polygonal approximation Γ_h of the smooth original boundary Γ. The boundary nodes of the triangulation are placed exactly at the boundary Γ. Note that Γ_h is in general not smooth. Now, the exterior domain is semi–discretized as it is exemplarily shown in Fig. 2. Each boundary node is connected with a point at infinity by ray-like straight line. These rays are not allowed to intersect each other. This way, the exterior domain is decomposed into a finite number of segments.

Fig. 3 displays one segment cut from the whole domain. This subdomain is bounded by the vertical line $x = 0$ and the two lines

$$\begin{aligned} y_1(x) &= y_{10} - a_1 x \\ y_2(x) &= y_{20} + a_2 x, \quad \text{with} \quad a_1 + a_2 \geq 0\,. \end{aligned}$$

In order to obtain the discrete variational form of the Helmholtz equation in the exterior domain, (1) is multiplied with a test function $v(x, y)$ and

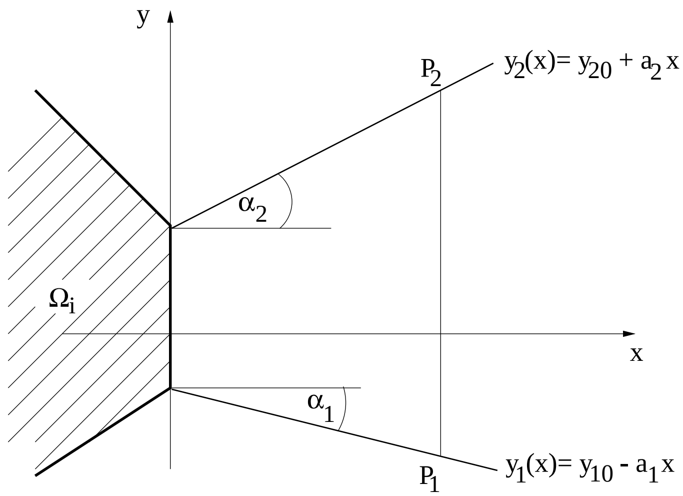

Figure 3: Definition of $y_1(x)$ and $y_2(x)$ as continuation of the boundary nodes

integrated by parts. Suppose the integration is performed between the points $P_1 = (x_1, y_1)$ and $P_2 = (x_2, y_2)$, i. e. , along the *transversal* coordinate. The corresponding equation for this special integration path is

$$\int_{P_1}^{P_2} \bar{v}(x,y)\partial_x^2 u(x,y)\, dy + \int_{P_1}^{P_2} \bar{v}(x,y)\partial_y^2 u\, dy + \int_{P_1}^{P_2} \bar{v}(x,y) n^2 k_0^2 u\, dy = 0\,. \tag{2}$$

Next we approximate the unknown function $u(x,y)$ in the exterior subdomain by means of functions $\tilde{u}_1(x, y_1(x)) = u_1(x)$ and $\tilde{u}_2(x, y_1(x)) = u_2(x)$ defined along the lines $y_1(x)$ and $y_2(x)$ and appropriate ansatz functions $v(x,y)$. Corresponding to finite element discretization of the interior domain we choose

$$\begin{aligned} v_1(x,y) &= \frac{y_2(x) - y}{h(x)} \\ v_2(x,y) &= \frac{y - y_1(x)}{h(x)} \\ h(x) &= y_2(x) - y_1(x)\,. \end{aligned}$$

Next, we define the discrete approximation of $u(x,y)$ in the subdomain between $y_1(x)$ and $y_2(x)$, which we will denote by $u_h(x,y)$,

$$u_h(x,y) = v_1(x,y)u_1(x) + v_2(x,y)u_2(x)\,.$$

The unknown functions $u_1(x)$ and $u_2(x)$ are solutions of a system of ordinary differential equations, which we will derive in the following. To this end, we will investigate (2) term by term. In order to simplify the notation we will abbreviate the path integration $\int \bar{v}u\,dy$ by (v,u) and the partial derivatives $\partial_x u(x,y)$ by u_x etc. Replacing $u(x,y)$ by $u_h(x,y)$ and choosing $v \in \{v_1(x,y), v_2(x,y)\}$, we obtain the local finite element matrix corresponding to the first term of (2)

$$\int_{P_1}^{P_2} \bar{v}(x,y)\partial_x^2 u(x,y)\,dy \longrightarrow \underbrace{\begin{pmatrix} (v_1,v_1) & (v_1,v_2) \\ (v_2,v_1) & (v_2,v_2) \end{pmatrix}}_{\mathbf{M}(x)} \begin{pmatrix} u_{1xx} \\ eu_{2xx} \end{pmatrix} + \\ 2\underbrace{\begin{pmatrix} (v_1,v_{1x}) & (v_1,v_{2x}) \\ (v_2,v_{1x}) & (v_2,v_{2x}) \end{pmatrix}}_{\mathbf{M}_x} \begin{pmatrix} u_{1x} \\ u_{2x} \end{pmatrix} + \underbrace{\begin{pmatrix} (v_1,v_{1xx}) & (v_1,v_{2xx}) \\ (v_2,v_{1xx}) & (v_2,v_{2xx}) \end{pmatrix}}_{\mathbf{M}_{xx}(x)} \begin{pmatrix} u_1 \\ u_2 \end{pmatrix} . \quad (3)$$

A straightforward computation yields the local element matrices

$$\begin{aligned} \mathbf{M}(x) &= \frac{h(0)+(a_1+a_2)x}{3} \begin{pmatrix} 1 & \frac{1}{2} \\ \frac{1}{2} & 1 \end{pmatrix} \quad (4) \\ \mathbf{M}_x &= \frac{1}{6} \begin{pmatrix} -2a_1+a_2 & 2a_1-a_2 \\ -a_1+2a_2 & a_1-2a_2 \end{pmatrix} \\ \mathbf{M}_{xx}(x) &= \frac{a_1+a_2}{3(h(0)+(a_1+a_2)x)} \begin{pmatrix} 2a_1-a_2 & -2a_1+a_2 \\ a_1-2a_2 & -a_1+2a_2 \end{pmatrix} . \end{aligned}$$

Note that the matrix $\mathbf{M}_x$ does not depend on the distance variable x. Next, we investigate the second term of (2). An integration by parts supplies

$$\int_{P_1}^{P_2} \bar{v}(x,y)\partial_y^2 u(x,y)\,dy \longrightarrow \begin{pmatrix} \bar{v}_1(x,y_1(x))\,\partial_y u_h(x,y)\big|_{y=y_1(x)} \\ \bar{v}_2(x,y_2(x))\,\partial_y u_h(x,y)\big|_{y=y_2(x)} \end{pmatrix} - \\ \underbrace{\begin{pmatrix} (v_{1y},v_{1y}) & (v_{1y},v_{2y}) \\ (v_{2y},v_{1y}) & (v_{2y},v_{2y}) \end{pmatrix}}_{\mathbf{S}_e(x)} \begin{pmatrix} u_1 \\ u_2 \end{pmatrix} . \quad (5)$$

The matrix $\mathbf{S}_e(x)$ is the conventional elementary stiffness matrix for the 1D Laplace operator. The subscript e stands for *edge* and means that this elementary stiffness matrix corresponds to the edge of the boundary, which bounds the related exterior segment. Evaluating the path integrals, we obtain

$$\mathbf{S}_e(x) = \frac{1}{h(0)+(a_1+a_2)x} \begin{pmatrix} 1 & -1 \\ -1 & 1 \end{pmatrix} . \quad (6)$$

Unlike in situations with smooth boundaries, where the boundary terms of the first term on the right hand side of (5) cancel each other after assembling of the system matrices, these terms do not vanish in our situation of a polygonal shaped boundary. For an approximate evaluation of these terms, let us consider the point $P_2 = (x_2, y_2)$. We have

$$\begin{aligned} v(x,y)\partial_y u_h(x,y)\big|_{y=y_2(x)} &= v(x, y_2(x))\partial_y u_h(x,y)\big|_{y=y_2(x)} \\ &= \partial_y u_h(x,y)\big|_{y=y_2(x)} \\ &= \nabla u(x,y)\big|_{y=y_2(x)} \, \mathbf{e_y} \\ &= \nabla u(x,y)\big|_{y=y_2(x)} \left(\sin\alpha_2 \, \mathbf{e}_r + \cos\alpha_2 \, \mathbf{e}_t\right) . \end{aligned}$$

Here $\mathbf{e}_y$ is the unit vector in the y-direction, $\mathbf{e}_r$ is the radial unit vector, parallel to $y_2(x)$, and $\mathbf{e}_t$ is the unit vector perpendicular to $\mathbf{e}_r$, i. e. , $\mathbf{e}_r \cdot \mathbf{e}_t = \mathbf{0}$, and we have expressed the Cartesian unit vector $\mathbf{e}_y$ by the radial and tangential unit vectors. From these terms we need to consider only the radial part, because the tangential parts of two neighboring boundary elements cancel each other. Suppressing the tangential part, it follows

$$\partial_y u_h(x,y)\big|_{y=y_2(x)} = \sin\alpha_2 \left(\partial_x u_h \mathbf{e}_x \mathbf{e}_r + \partial_y u_h \mathbf{e}_y \mathbf{e}_r\right) .$$

The polygonal shaped boundary serves as an approximation of the smooth boundary of the original domain. Therefore, the finer the triangulation and the larger the local bending radii of the original boundary the smaller becomes α_2. Thus, we find approximately,

$$\mathbf{e}_x \mathbf{e}_r \to 1 \qquad \text{and} \qquad \mathbf{e}_y \mathbf{e}_r \to 0 \, .$$

Further, in the limit of a small angle α_2, we can replace $\partial_x u_h(x,y)$ at $y = y_2(x)$ by $\partial_x u_2(x)$ and $\sin\alpha_2$ by a_2. Altogether, we find the finite element approximation

$$\int_{P_1}^{P_2} \bar{v}(x,y)\partial_y^2 u(x,y)\, dy \longrightarrow \mathbf{S}_\alpha \begin{pmatrix} u_{1x} \\ u_{2x} \end{pmatrix} - \mathbf{S}_e(x) \begin{pmatrix} u_1 \\ u_2 \end{pmatrix} ,$$

with

$$\mathbf{S}_\alpha = \begin{pmatrix} a_1 & 0 \\ 0 & a_2 \end{pmatrix} ,$$

and $\mathbf{S}_e(x)$ given by (6). The subscript α has been chosen to indicate that this part of the boundary stiffness matrix originates from the angles between two neighboring boundary elements.

The last term of (2) again represents a mass-term which is weighted by the constant coefficient $n^2k_0^2$. Hence, we obtain, in analogy to the computation of the first term and with the matrix $\mathbf{M}(x)$ defined in (4),

$$\int_{P_1}^{P_2} \bar{v}(x,y)n^2k_0^2 u\,dy \longrightarrow n^2k_0^2\,\mathbf{M}(x)\begin{pmatrix} u_1 \\ u_2 \end{pmatrix} .$$

Next, we assemble the whole system of ordinary differential equations. In order to maintain a suggestive notation and to avoid the introduction of new symbols, we use for the assembled large matrices the same symbols as for the local matrices. The only exception is the labeling of the weighted mass matrix. Since the factors $n^2k_0^2$ may be different in each of the exterior segments, we label the assembled weighted mass matrix by $\mathbf{M}_w(x)$. Further, we continue to use the variable x as the distance variable. The resulting system reads now

$$\mathbf{M}(x)\mathbf{u}_{xx} + (2\mathbf{M}_x + \mathbf{S}_\alpha)\mathbf{u}_x + \big(\mathbf{M}_{xx}(x) + \mathbf{M}_w(x) - \mathbf{S}_e(x)\big)\mathbf{u} = 0\,. \qquad (7)$$

4 Discrete boundary operator

Besides the approximation with respect to $\mathbf{S}_\alpha$, where we have exploited the assumption of large local bending radii, (7) is exact. The main approximation step is now to neglect the x-dependence of the matrices $\mathbf{M}(x)$, $\mathbf{M}_w(x)$, $\mathbf{M}_{xx}(x)$, $\mathbf{S}_e(x)$, and to replace them by $\mathbf{M}(0)$, $\mathbf{M}_w(0)$, $\mathbf{M}_{xx}(0)$, $\mathbf{S}_e(0)$. This approximation allows for an elementary derivation of an asymptotic correct boundary operator $\mathbf{B}$. The approximation becomes the better the larger the local bending radii, hence, the larger the computational domain. Using this asymptotic approximation, (7) simplifies to a system of ordinary differential equations with constant coefficients

$$\mathbf{M}(0)\mathbf{u}_{xx} + (2\mathbf{M}_x + \mathbf{S}_\alpha)\mathbf{u}_x + \mathbf{M}_{xx}(0) + \mathbf{M}_w(0) - \mathbf{S}_e(0)\mathbf{u} = 0\,. \qquad (8)$$

To simplify the notation, we write from now $\mathbf{M}$ instead of $\mathbf{M}(0)$, etc. A Laplace transformation of (8), which results in

$$\big[\mathbf{M}p^2 + (2\mathbf{M}_x + \mathbf{S}_\alpha)p + \mathbf{M}_{xx} + \mathbf{M}_w - \mathbf{S}\big]\,\mathbf{u}(p) = \\ \mathbf{M}(p\mathbf{u}_0 + \mathbf{u}_{0x}) + (2\mathbf{M}_x + \mathbf{S}_\alpha)\mathbf{u}_0\,, \qquad (9)$$

yields directly a solution for the dual variable $\mathbf{u}(p)$ with $p \in \mathbf{C}, \Re(p) \geq 0$. The matrix $\mathbf{M}$ in (9) is symmetric positive definite, hence invertible, and (9) can be rewritten as

$$\begin{aligned}
\left(\mathbf{I}p^2 + \mathbf{C}p + \mathbf{D}\right)\mathbf{u}(p) &= p\mathbf{u}_0 + \mathbf{u}_{0x} + \mathbf{C}\mathbf{u}_0 && (10)\\
\text{with}\quad \mathbf{C} &= \mathbf{M}^{-1}\left(2\mathbf{M}_x + \mathbf{S}_\alpha\right) && (11)\\
\mathbf{D} &= \mathbf{M}^{-1}\left(\mathbf{M}_{xx} + \mathbf{M}_w - \mathbf{S}\right). && (12)
\end{aligned}$$

Further, let us introduce the boundary operator $\mathbf{B}$ by

$$\mathbf{M}\mathbf{u}_{0x} = \mathbf{B}\mathbf{u}_0\,.$$

Equation (10) now takes the simple form

$$\left(\mathbf{I}p^2 + \mathbf{C}p + \mathbf{D}\right)\mathbf{u}(p) = \left(\mathbf{I}p + \mathbf{M}^{-1}\mathbf{B} + \mathbf{C}\right)\mathbf{u}_0\,. \tag{13}$$

With a factorization of the quadratic expression on the left-hand side of (13)

$$\left(\mathbf{I}p^2 + \mathbf{C}p + \mathbf{D}\right) = \left(\mathbf{I}p - \mathbf{F}_-\right)\left(\mathbf{I}p - \mathbf{F}_+\right) \tag{14}$$

the solution becomes

$$\mathbf{u}(p) = \left(\mathbf{I}p - \mathbf{F}_+\right)^{-1}\left(\mathbf{I}p - \mathbf{F}_-\right)^{-1}\left(\mathbf{I}p + \mathbf{M}^{-1}\mathbf{B} + \mathbf{C}\right)\mathbf{u}_0\,.$$

The subscripts $\pm$ indicate that the the eigenvalues λ of the matrices $\mathbf{F}_\pm$ have only positive (negative) imaginary parts. The real part of all eigenvalues is always nonpositive. The special choice of the boundary operator

$$\mathbf{B} = -\mathbf{M}\left(\mathbf{C} + \mathbf{F}_-\right) \tag{15}$$

yields the corresponding solution

$$\mathbf{u}(p) = \left(\mathbf{I}p - \mathbf{F}_+\right)^{-1}\mathbf{u}_0\,. \tag{16}$$

Since $\Re(\lambda(F_+)) \le 0$ and $\Im(\lambda(F_+)) > 0$, (16) contains only non-increasing and outgoing modes. Hence $\mathbf{B}$, given by (15), is the desired boundary operator.

It remains to find a suitable approximation of $\mathbf{F}_-$. The matrix $\mathbf{F}_-$ is a solution of a quadratic matrix equation. There are some iterative methods to solve such matrix equations, including Newton's method and iterations of the algebraic Ricatti equation, see e. g. [12]. The application of these methods, however, causes additional numerical effort, therefore we try to find approximations $\widetilde{\mathbf{F}}_\pm$ of $\mathbf{F}_\pm$ by

$$\widetilde{\mathbf{F}}_\pm = -\frac{1}{2}\mathbf{C} \pm \frac{1}{2}\left(\mathbf{C}^2 - 4\mathbf{D}\right)^{1/2}\,,$$

which is motivated by the corresponding scalar quadratic equation. Clearly, this causes an error

$$\left(\mathbf{I}p - \widetilde{\mathbf{F}}_-\right)\left(\mathbf{I}p - \widetilde{\mathbf{F}}_+\right) - (\mathbf{I}p - \mathbf{F}_-)(\mathbf{I}p - \mathbf{F}_+) = \frac{1}{4}\left((\mathbf{C}^2 - 4\mathbf{D})^{1/2}\mathbf{C} - \mathbf{C}(\mathbf{C}^2 - 4\mathbf{D})^{1/2}\right)$$

in the constant term of the quadratic expression. In the asymptotic case, however, when the bending radii become large, $\mathbf{C}$ tends to zero and the error term vanishes. Hence, our factorization is asymptotic correct. This way, we obtain a first version of the boundary operator,

$$\mathbf{B} = -\mathbf{M}\left(\frac{1}{2}\mathbf{C} - \frac{1}{2}(\mathbf{C}^2 - 4\mathbf{D})^{1/2}\right). \tag{17}$$

Numerical experience shows that a further simplification, concerning the square-root expression involved in (17), is sufficient for many problems. To derive this approximation, we employ the asymptotic properties $|\mathbf{C}| \ll |\mathbf{D}|$ and $|\mathbf{M}_{xx}| \ll |\mathbf{M}_w|$, where the inequalities hold componentwise, and which is valid for large local bending radii of the boundary. Additionally, we know that the mass matrices $\mathbf{M}$ and $\mathbf{M}_w$ are close to diagonal matrices. In fact, for the numerical realization of the boundary operator we use throughout the lumped, hence diagonal, approximation of the original mass matrices. Thus the numerical approximations of $\mathbf{M}$ and $\mathbf{M}_w$ commute with each other. Using these properties, the boundary operator reads

$$\mathbf{B} = -\mathbf{M}\left(\frac{1}{2}\mathbf{C} - i\left[\mathbf{M}^{-1}(\mathbf{M}_w - \mathbf{S}_e)\right]^{1/2}\right). \tag{18}$$

To understand this equation, it is useful to consider the special case of a homogeneous exterior domain, i. e. $\mathbf{M}_w = n^2k_0^2\mathbf{M}$, and a solution $\mathbf{u}$, which is constant along the boundary, i. e. , $\mathbf{S}_e\mathbf{u} \to \mathbf{0}$. The resulting boundary operator is simply

$$\mathbf{B}_S = -\frac{1}{2}\mathbf{M}\mathbf{C} + in_0k_0\mathbf{M}. \tag{19}$$

The matrix $1/2\mathbf{MC}$ is approximately a diagonal matrix and contains entries of the type $const./r$, with r the local bending radius of the boundary. Hence, we have recovered a discrete Sommerfeld-like boundary condition. Keeping this Sommerfeld-like radiation condition in mind, we approximate the square-root in (18) such that we take the matrix $\mathbf{M}_w$ as dominant term and the stiffness matrix $\mathbf{S}_e$ as perturbation. In other words, the task, which we want to solve approximately, is to find a matrix $\mathbf{X}$, such that

$$\mathbf{X}^2 = \mathbf{A}^2 + \mathbf{P}\,,$$

with a dominant matrix $\mathbf{A}^2$ and a small perturbation $\mathbf{P}$. We suggest an approximate solution

$$\mathbf{X} = \mathbf{A} + \frac{1}{2}\mathbf{A}^{-1}\mathbf{P}\,,$$

which can be seen as the first iterate of the Newton-like iteration

$$\mathbf{X}_{k+1} = \frac{1}{2}\left(\mathbf{X}_k + \mathbf{X}_k^{-1}(\mathbf{A}^2 + \mathbf{P})\right)\,, \quad \mathbf{X}_0 = \mathbf{A}, \quad k = 0, 1 \ldots .$$

In fact, this iteration is different from Newton's method, which would involve the solution of Sylvester's equation. Since we want to derive only a lowest order correction without any additional computational effort, we have restricted ourselves to this simplified iteration. Applying this square-root approximation to (18), we obtain finally

$$\mathbf{B} = -\frac{1}{2}\left(2\mathbf{M}_x + \mathbf{S}_\alpha\right) + i\mathbf{M}^{1/2}\left(\mathbf{M}_w^{1/2} - \frac{1}{2}\mathbf{M}_w^{-1/2}\mathbf{S}_e\right)\,. \qquad (20)$$

5 Application

In preparation of the numerical reflection experiment, we compute first the propagation of a Gaussian beam in a homogeneous medium. The computational domain (see Fig.'s 1 and 2) has an extension of $3\,\mu m \times 3\,\mu m$. The refractive index of this domain is $n = 3.2$, the wavelength $\lambda = 1.55\,\mu m$. The waveguide supports a fundamental mode of Gaussian profile with an 1/e-width of $0.54\mu m$. Fig. 4 displays the result of the simulation in terms of iso-curves with respect to $|u(x, y)|$. The smoothness of these iso-curves can be seen as an indicator for the quality of the boundary conditions. The inner rectangle marks the position, where we will insert the dielectric mirror in a later experiment. The smoothness of the iso-curves in Fig. 4 shows that the derived discrete boundary operator (20) works well.

Next, we show that this boundary operator, in fact, supplies better results than the discrete Sommerfeld-like boundary condition, which is obtained by setting $\mathbf{S}_\alpha = \mathbf{S}_e = \mathbf{M}_x = \mathbf{0}$. The corresponding simulation run is documented in Fig. 5. The wave-like behavior of the iso-curves, especially near the corners, indicate that a non-neglectable amount of reflection is generated at the boundary.

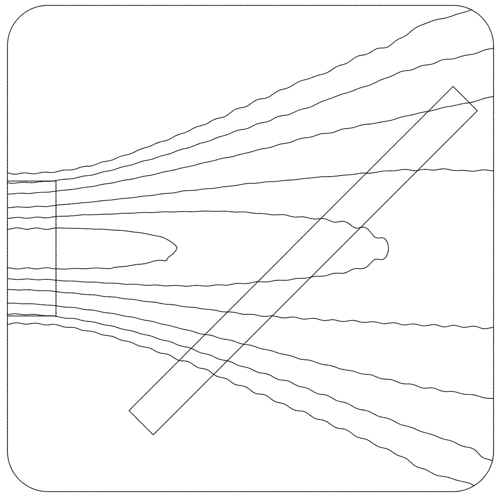

Figure 4: Iso-curves of $|u(x, y)|$ of a Gaussian beam propagating in a homogeneous medium, computed with the discrete boundary operator. The levels of the iso-curves are taken to $\max(|u|)\,\{0.8,\ 0.6,\ 0.4,\ 0.2,\ 0.1, 0.05\}$. The inner rectangle indicates the position of a mirror for the following numerical experiments.

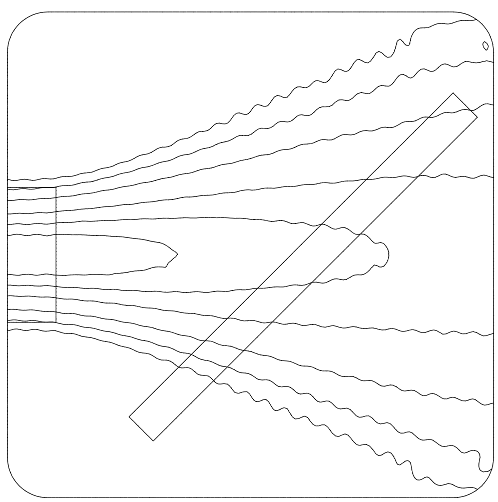

Figure 5: Iso-curves of $|u(x, y)|$ of a Gaussian beam propagating in a homogeneous medium, computed with the Sommerfeld-like approximation of the boundary operator. The levels of the iso-curves are the same as in Fig. 4. Residual reflections occur.

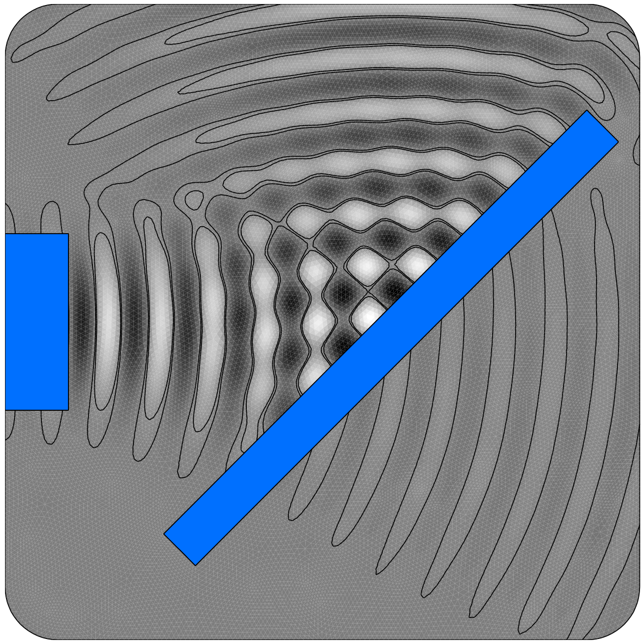

Figure 6: Iso-curves of the solution $\Re(u)$ displaying the typical interference pattern

In a second experiment, we insert the dielectric mirror. The mirror has a thickness of $0.3\,\mu m$ and a refractive index $n = 1.5$. These parameters has been chosen such that diffraction and refraction occur, too. Fig. 6 shows the real part of the field distribution. It displays the typical interference pattern of reflected waves. Further, the refracted part of the wave becomes visible.

Another representation of the same field is given in Fig. 7, which shows the intensity distribution of the reflected field. Here, we take the intensity to $I(x, y) = |\Re(i\bar{u}\nabla u)|$. It is apparent from these figures that the direct simulation of the Helmholtz equation equipped with transparent boundary conditions supplies a useful tool in studying of reflection phenomena.

6 Conclusions

We have derived an asymptotic discrete transparent boundary condition for the Helmholtz equation with inhomogeneous exterior domain. Our derivation is not restricted to a special choice of a coordinate system. The central assumption, which we have made, is that the local bending radii of the boundary of the computational domain are sufficiently large. For practical

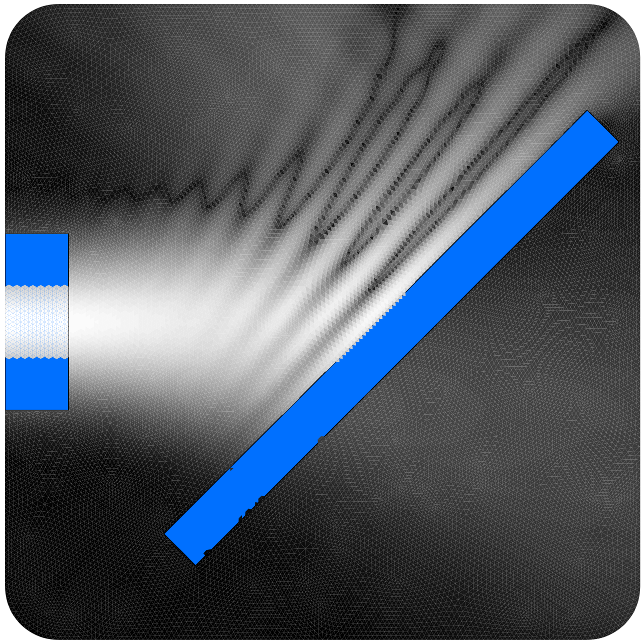

Figure 7: Intensity distribution of the reflected beam

purposes this means that the bending radii must be of the order of the local wavelength. The smoother the boundary and the larger the interior domain the better the approximation. Numerical experiments validate the efficiency of the discrete boundary operator.

Acknowledgment

The author acknowledges the encouragement and continuous support by P. Deuflhard.

References

[1] G. R. Hadley. Numerical simulation of reflecting structures via solution of the 2D Helmholtz equation. In *Integrated Photonics Research*, volume 3, pages ThD1–1, San Francisco, California, February 17-19 1994.

[2] W. P. Huang, S. T. Chu, A. Goss, and S. K. Chaudhuri. *IEEE Phot. Tech. Lett.*, 3(6):524, 1991.

[3] A. Sommerfeld. *Lectures on Theoretical Physics*, volume 6 (Partial Differential Equations), chapter 28. Academic Press, 1964.

[4] D. Givoli. *Numerical methods for problems in infinite domains*, volume 33 of *Studies in Applies Mechanics*. Elsevier, 1992.

[5] M. J. Grote and J. B. Keller. On nonreflecting boundary conditions. *J. Comput. Phys*, 122:231–243, 1995.

[6] A. Bayliss, M. Gunzburger, and E. Turkel. Boundary conditions for the numerical solution of elliptic equations in exterior domains. *SIAM J. Appl. Math.*, 42:430–451, 1982.

[7] K. Gerdes. Asummary of infinite element formulations for exterior Helmholtz problems. Technical Report 97-11, Seminar für Angewandte Mathematik, ETH Zürich, August 1997.

[8] S. Amini and S. M. Kirkup. Solution of Helmholtz equation in the exterior domain by elementary boundary integral methods. *J. Comput. Phys.*, 118:208–221, 1995.

[9] C. I. Goldstein. A finite-element method for solving Helmholtz type equations in waveguides and other unbounded domains. *Math. of Comput.*, 39, 1982.

[10] F. Schmidt and P. Deuflhard. Discrete transparent boundary conditions for the numerical solution of Fresnel's equation. *Computers Math. Applic.*, 29:53–76, 1995.

[11] F. Schmidt and D. Yevick. Discrete transparent boundary conditions for Schrödinger-type equations. *J. Comput. Phys.*, 134:96–107, 1997.

[12] Nicholas J. Higham. Newton's method for the matrix square root. *Math. Comp.*, 46(174):537–549, April 1986.